

ENERGY DEPENDENCE OF INELASTIC PROTON SCATTERING TO ONE-PARTICLE ONE-HOLE STATES IN  $^{28}\text{Si}$

C. Olmer, A.D. Bacher, G.T. Emery, W.P. Jones, D.W. Miller, and P. Schwandt  
Indiana University Cyclotron Facility, Bloomington, Indiana 47405

S. Yen, T.E. Drake, and R.J. Sobie  
University of Toronto, Toronto, Ontario, Canada

The study of intermediate-energy proton inelastic scattering to one-particle one-hole states has attracted considerable attention over the last few years. One primary purpose of these studies has been to exploit the structural simplicity of these excited states as a possible means of separating effects due to nuclear structure and those due to the reaction mechanism. The present work has concentrated on an examination of the energy dependence of the proton inelastic excitation of three high-spin, particle-hole states in  $^{28}\text{Si}$ : the  $5^-$ ,  $T=0$  state at 9.70 MeV, the  $6^-$ ,  $T=0$  state at 11.58 MeV and the  $6^-$ ,  $T=1$  state at 14.35 MeV. A region of the inelastic scattering spectrum measured at an incident energy of 180 MeV is displayed in Fig. 1. These high-spin states in  $^{28}\text{Si}$  have been particularly useful in proton inelastic scattering

studies since: (1) the states usually appear as strong, isolated peaks in the spectrum, (2)  $^{28}\text{Si}$  is a self-conjugate nucleus so that differences between proton and neutron transition densities are not expected to be a problem, and (3) all three states have also been studied by pion inelastic scattering<sup>1</sup> and the  $5^-$ ,  $T=0$  and  $6^-$ ,  $T=1$  states have been studied by electron inelastic scattering<sup>2</sup>, so that this is one of the few cases for which  $p-\pi-e$  complementary information exists.

The distorted-wave impulse approximation (DWIA) description of inelastic scattering to these states incorporates information concerning the nuclear wave functions of the states, the effective N-N interaction and  $p-^{28}\text{Si}$  elastic scattering distorted waves. The elastic scattering data measured at the various energies are displayed in Fig. 2. It is extremely important in a study of the energy dependence of inelastic scattering to measure both the cross section  $\sigma$  and the analyzing power  $A$  for the elastic scattering over a wide range of both proton energy  $E_p$  and momentum transfer  $q$ . In the present study, a standard Woods-Saxon optical-model description of the elastic scattering was employed, and the resulting energy dependence of the deduced optical model parameters was investigated. By requiring a smooth dependence on  $E_p$  for these parameters (including the total reaction cross section), a significant reduction in the ambiguity of parameters was possible. The use of a non-standard optical potential (Woods-Saxon plus a squared Woods-Saxon term), which was found<sup>3</sup> to be important for reproducing proton elastic scattering

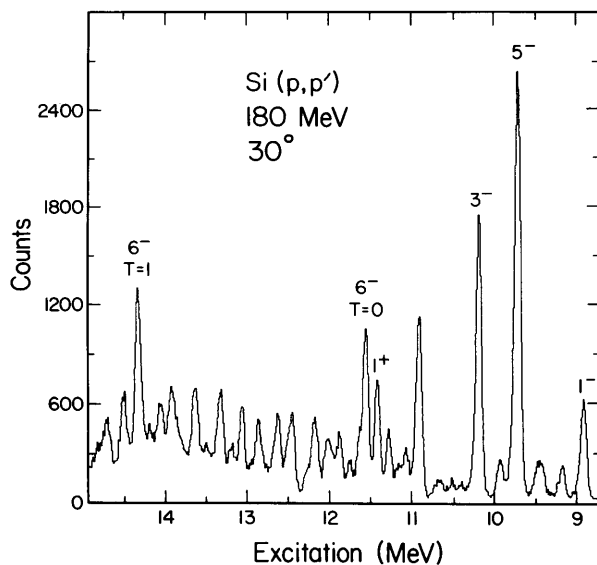


Figure 1. Inelastic proton spectrum for the scattering of 180 MeV protons from silicon.

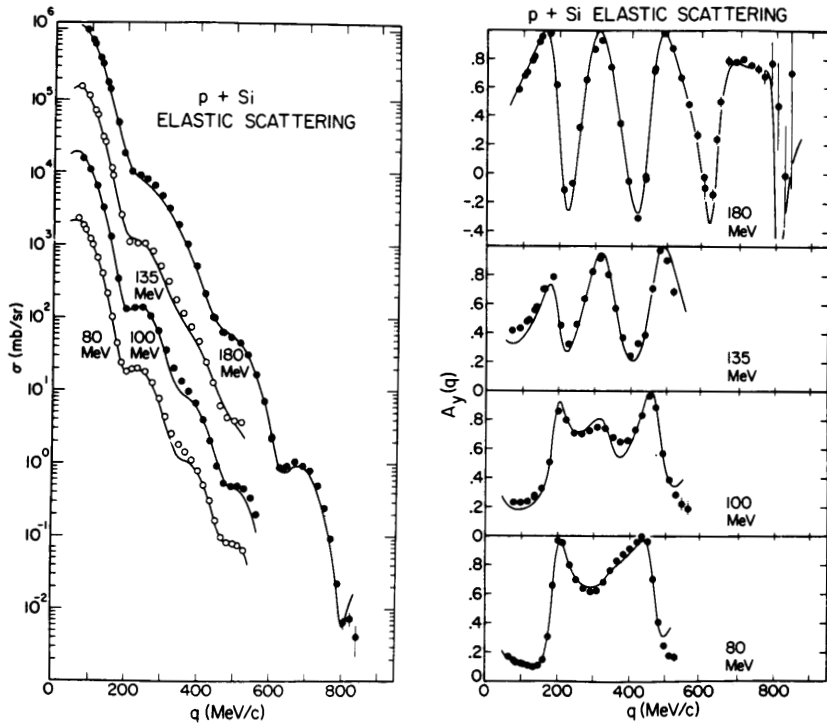


Figure 2. Momentum transfer dependence of the cross sections and analyzing powers for proton elastic scattering by silicon. The curves are the results of simultaneous optical-model fits to the cross section and analyzing power data at each energy.

from light nuclei, did not significantly affect the quality of the optical model fit at 180 MeV. This potential resulted in inelastic scattering analyzing-power predictions of similar shape and magnitude, and cross-section predictions of similar shape and slightly different magnitude as compared to the standard optical model treatment. A detailed description of the elastic scattering analysis will be presented elsewhere.<sup>4</sup>

The wave functions of the three states have been assumed to be of harmonic oscillator form, and the oscillator parameters derived from  $(e, e')$  studies<sup>2</sup> of the  $5^-$ ,  $T=0$  and  $6^-$ ,  $T=1$  transitions have been used ( $b=1.91$  and  $b=1.74$ , respectively). The  $6^-$ ,  $T=0$  state is assumed to have the same oscillator parameter as the  $6^-$ ,  $T=1$  state. Both  $6^-$  states are characterized by the  $f_{7/2}d_{5/2}^{-1}$  configuration, whereas the  $5^-$ ,  $T=0$  state is

described by an RPA wave function,<sup>5</sup> which has a dominant  $f_{7/2}d_{3/2}^{-1}$  term.

Several different effective interactions have been considered in this study. These include:

- (1) the Love-Franey interaction<sup>6</sup> (LF), which has been separately derived at 100, 140 and 185 MeV,
- (2) The Geramb-Bauhoff interaction<sup>7</sup> (GB), which is a density-dependent interaction based on the Paris N-N interaction and is available at isolated energies (also the Hamada-Johnston<sup>8</sup> interaction (HJ), which is available for central and spin-orbit components only), and
- (3) the Picklesimer-Walker interaction<sup>9</sup> (PW), which explicitly incorporates both energy and momentum dependence.

The DWIA calculations employing the LF and PW

interactions used the code DW81<sup>10</sup> and those employing the GB interaction used the code DWBA80.<sup>11</sup> All calculations treated the exchange term in an exact manner.

Several different types of comparisons of the model predictions with the data have been examined, including: (1) the dependence of the maximum cross section  $\sigma_{\max}$  on  $E_p$ , (2) the dependence of the differential cross section  $\sigma$  on  $E_p$  and  $q$ , and (3) the dependence of the analyzing power  $A$  on  $E_p$  and  $q$ . A complete discussion of the results of these comparisons is presented elsewhere.<sup>12</sup>

The simplest possible comparison of the DWIA predictions with the data involves the energy dependence of  $\sigma_{\max}$ , since it ignores the dependence on the momentum transfer. The experimental values of  $\sigma_{\max}$  for the  $5^-$ ,  $T=0$  and  $6^-$ ,  $T=0$  transitions are displayed in Fig. 3, together with predictions based on the various interactions. (An additional set of calculations is displayed, using an earlier form<sup>13</sup> of the Love interaction derived at 135 MeV. Also, note that the LF results are displayed only for energies of 100 MeV and above). The individual contributions of direct and exchange are displayed, and these vary dramatically for the various interactions. These terms interfere constructively for some interactions and destructively for others. For some interactions, very different direct and exchange terms combine to produce very similar predictions. Experimentally, the energy dependences of  $\sigma_{\max}$  for these two transitions are very similar. Only the LF calculations seem to reproduce this observation, whereas the GB and PW calculations predict significantly different dependences on proton energy. Clearly an analysis over a broader range of energy is necessary in order to verify these conclusions.

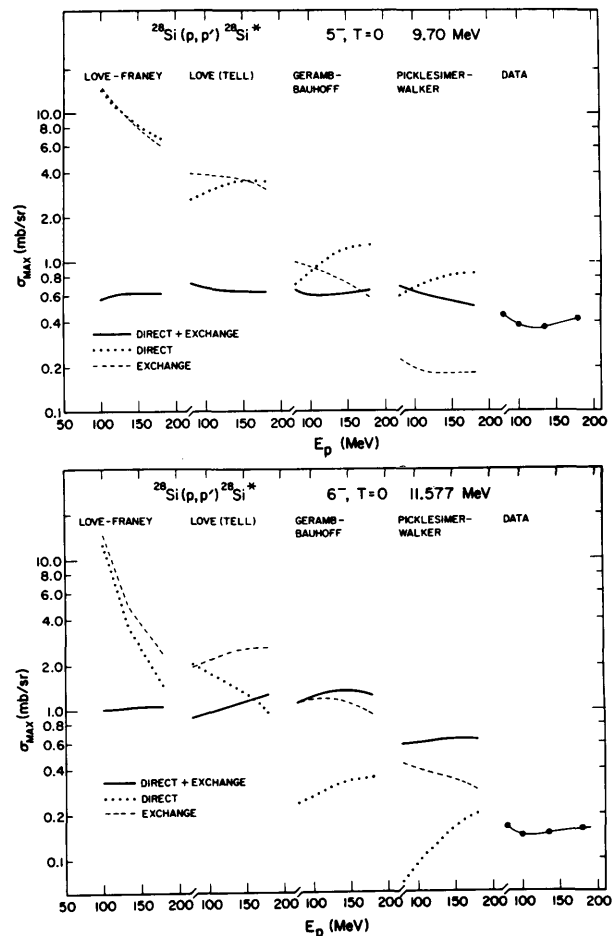


Figure 3. Energy dependence of the maximum cross sections for proton inelastic excitation of the  $5^-$ ,  $T=0$  and  $6^-$ ,  $T=0$  states in  $^{28}\text{Si}$ . For the data, a smooth curve has been drawn through the four experimental measurements for each transition.

A further comparison can be made by examining the renormalization factors, shown in Fig. 4, which are needed in order for these theoretical values of  $\sigma_{\max}$  to reproduce the data. For the  $5^-$ ,  $T=0$  transition, all renormalization factors for all the indicated interactions have a similar value and a relatively flat energy dependence is seen for these factors (with the exception of the PW interaction at high energies). As a result of these observations, it may be concluded that both the LF and GB interactions reproduce reasonably well the energy dependence of  $\sigma_{\max}$  for the

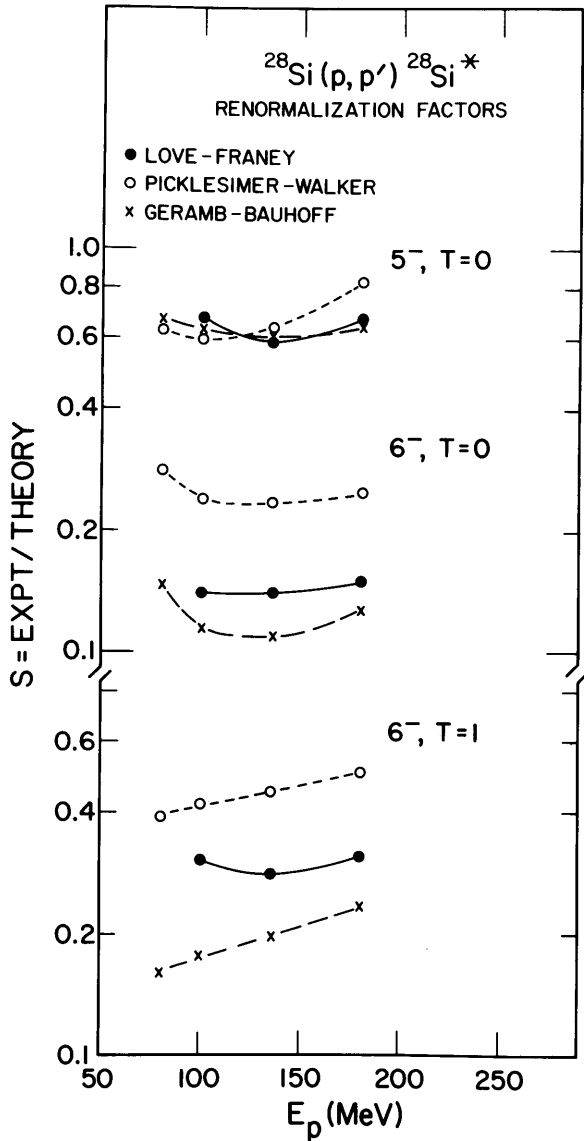


Figure 4. Energy dependence of the renormalization factors for proton inelastic excitation of the  $5^-, T=0$ ,  $6^-, T=0$  and  $6^-, T=1$  states in  $^{28}\text{Si}$ .

$5^-$  transition. For the  $6^-, T=1$  transition, only the LF interaction appears to require the same renormalization factor over the indicated range of proton energies and, moreover, the value of this factor is remarkably close to that obtained<sup>1,2</sup> in  $(e, e')$  and  $(\pi, \pi')$  studies. Calculations with all interactions indicate that this transition is dominated by the tensor component of the interaction. Thus it may be concluded that the

increase in strength of the tensor component in this energy region (100–200 MeV) is reproduced reasonably well by the LF interaction, but that the energy dependence of the tensor component in both the GB and PW interactions does not appear to be quite correct for this transition.

The energy and momentum-transfer dependences of  $\sigma$  and  $A$  for the three transitions have been examined for the various interactions. For example, the calculations for the  $5^-$  transitions using the LF and GB interactions are displayed, together with the data, in Fig. 5 and 6. The calculations have been renormalized by the factors indicated in the appropriate figure captions. (Calculations at 80 MeV for the LF interaction employed the 100 MeV force). The decomposition of the predicted cross section into central (C), spin-orbit (LS) and tensor (T) contributions is indicated for each of the interactions. Calculations using the LF interaction, shown in Fig. 5, appear to reproduce the energy dependence of  $\sigma_{\text{max}}$  and  $q_{\text{max}}$  (the location of  $\sigma_{\text{max}}$ ) reasonably well, but consistently fail to reproduce the width of the distributions. The predicted distributions are narrower than experimentally observed, and moreover, the calculations do not exhibit the observed increase in width of the distributions at the lower incident energies. Calculations for the  $5^-$  transition using the GB interaction, shown in Fig. 6, also appear to reproduce the energy dependence of  $\sigma_{\text{max}}$  and  $q_{\text{max}}$ , and here the calculations reproduce the experimental width of the distributions significantly better than was observed for the LF interaction. In particular, the shape of the distribution at 135 MeV is not exhibited in the LF calculation, but is well-reproduced in the GB calculation, where it results from the large, second maximum of the central

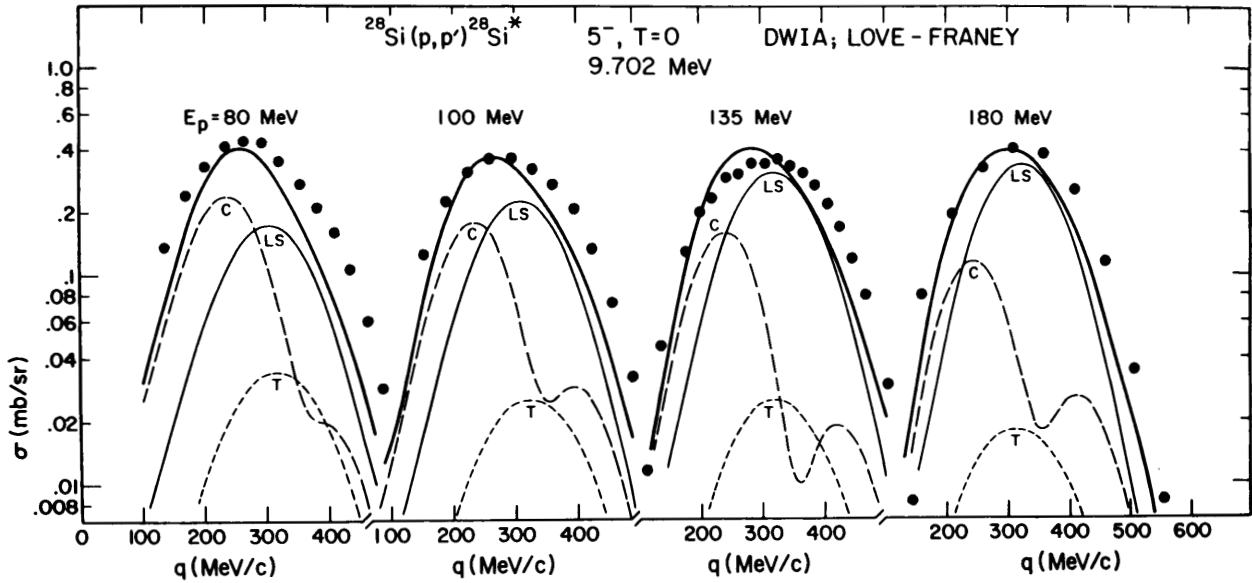


Figure 5. Momentum transfer dependence of the cross sections for proton inelastic excitation of the  $5^-$ ,  $T=0$  state at 9.70 MeV in  $^{28}\text{Si}$ . The curves are DWIA calculations (multiplied by 0.67) using the Love-Franey effective interaction and optical potentials appropriate for the various energies.

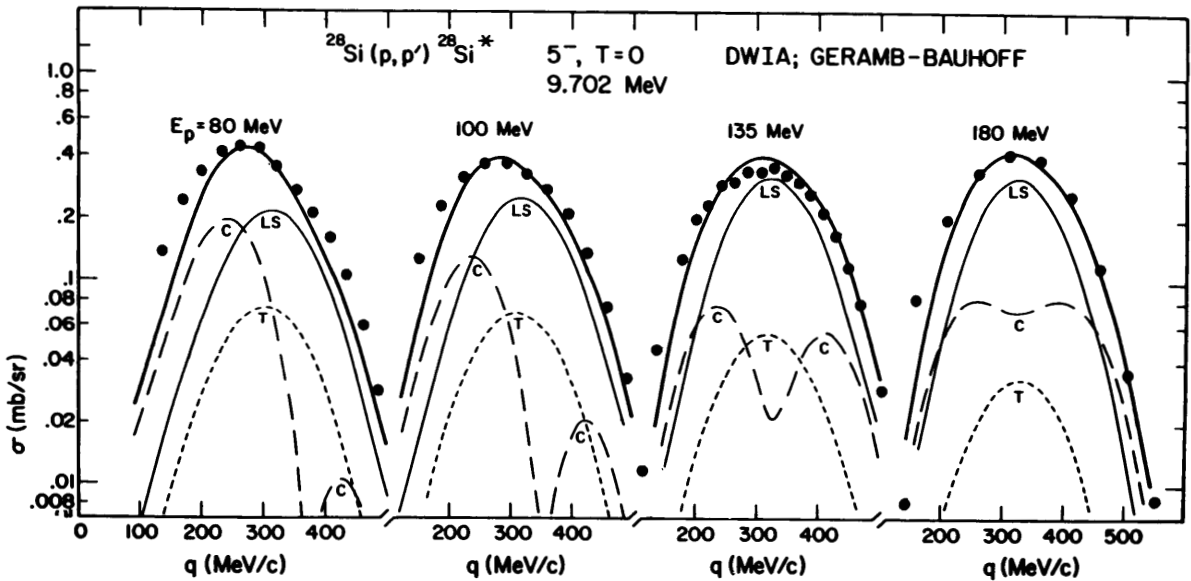


Figure 6. Momentum transfer dependence of the cross sections for proton inelastic excitation of the  $5^-$ ,  $T=0$  state at 9.70 MeV in  $^{28}\text{Si}$ . The curves are DWIA calculations (multiplied by 0.67) using the Geramb-Bauhoff effective interaction and optical potentials appropriate for the various energies.

component (very weak in the LF calculation) contribution to the large momentum transfer region. This broadening of the distributions also results from calculations using the HJ interaction. Both the GB and HJ interactions are density dependent, and both exhibit a double-humped central contribution for proton energies between 100 and 180 MeV. Thus it appears that density dependence is important for a complete understanding of this transition.

The analyzing-power distributions for the  $5^-$ ,  $T=0$  transition are shown in Fig. 7, together with predictions for the four interactions. The most positive value of  $A$  is observed to decrease from  $\sim 0.8$  at 180 MeV to near zero at 80 MeV, and this general trend is apparent in calculations for all the interactions. Since  $A$  is sensitive to the interference of amplitudes, a comparison of the predicted and observed analyzing powers provides an independent test

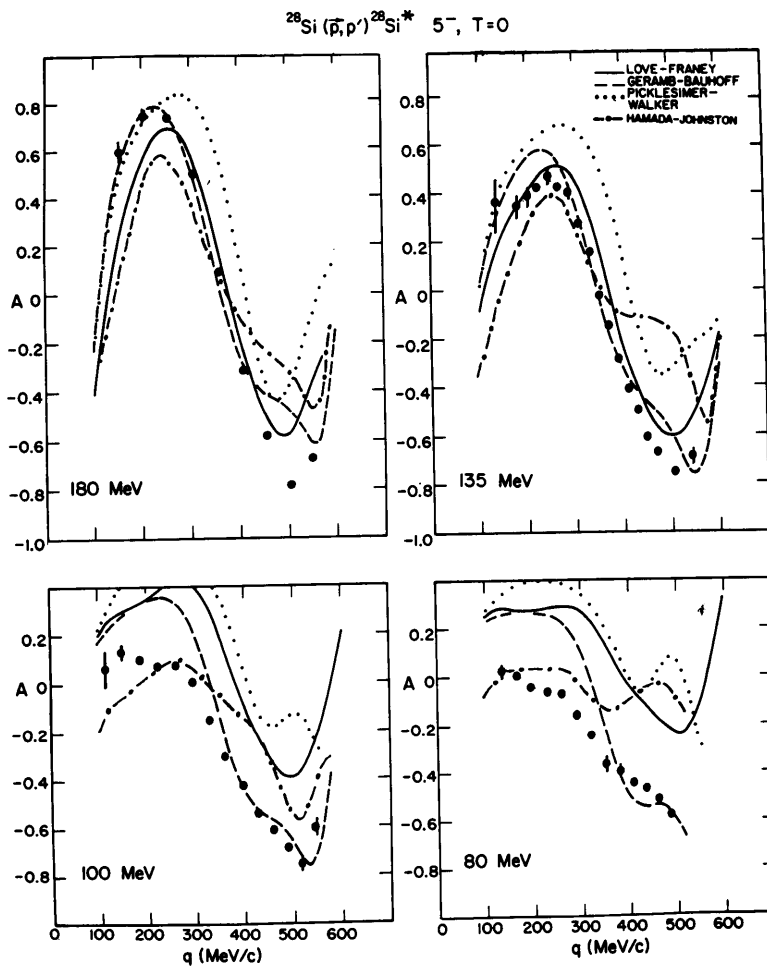


Figure 7. Momentum transfer dependence of the analyzing powers for proton inelastic excitation of the  $5^-$ ,  $T=0$  state at 9.70 MeV in  $^{28}\text{Si}$ .

of the interaction, separate from that furnished by the cross section. Here, both the GB and LF calculations are in reasonable agreement with the data, although the GB interaction appears to be slightly preferred.

The detailed comparisons of predictions based on various available effective interactions with inelastic scattering data over a broad range of incident energy has only recently become possible. The importance of such comparisons has become clear from the present study which has revealed information concerning the effective interaction which would normally be inaccessible for experiments and analyses at isolated energies.

- 1) C. Olmer, B. Zeidman, D.G. Geesaman, T-S. H. Lee, R.E. Segel, L.W. Swenson, R.L. Boudrie, G.S. Blanpied, H.A. Thiessen, C.L. Morris, and R.E. Anderson, Phys. Rev. Lett. 43, 612 (1979).
- 2) S. Yen, R.J. Sobie, H. Zarek, B.O. Pich, T.E. Drake, C.F. Williamson, S. Kowalski, and C.P. Sargent, Phys. Lett. 93B, 250 (1980); S. Yen, to be published.
- 3) H.O. Meyer, P. Schwandt, G.L. Moake, and P.P. Singh, Phys. Rev. C 23, 616 (1981).
- 4) C. Olmer, A.D. Bacher, G.T. Emery, W.P. Jones, D.W. Miller, P. Schwandt, T.E. Drake, R.J. Sobie, and S. Yen, to be published.
- 5) S. Yen, R.J. Sobie, T.E. Drake, A.D. Bacher, G.T. Emery, W.P. Jones, D.W. Miller, C. Olmer, P. Schwandt, W.G. Love, and F. Petrovich, Phys. Lett. 105B, 421 (1981); S. Yen, Ph.D. Thesis, University of Toronto (1983).
- 6) W.G. Love and M.A. Franey, Phys. Rev. C 24, 1073 (1981).
- 7) K. Nakano and H.V. von Geramb, Paris Potential, A Table of Effective Density and Energy Dependent Interactions; Central Spin-Orbit and Tensor Potentials, preprint, Universitat Hamburg (1982); M. Lacombe, B. Loiseau, R. Vinh Mau, J. Cote, P. Pines, and R. de Journeil, Phys. Rev. C 23, 2405 (1981).
- 8) H.V. von Geramb, Table of Effective Density and Energy Dependent Interactions for Nucleons, Part A: Central Potential; W. Bauhoff and H.V. von Geramb, Part B: Spin-Orbit Potential, preprint, Universitat Hamburg (1980); T. Hamada and I.D. Johnston, Nucl. Phys. 34, 382 (1962).
- 9) A. Picklesimer and G. Walker, Phys. Rev. C 17, 237 (1978).
- 10) R. Schaeffer and J. Raynal (unpublished); modified by J. Comfort.
- 11) R. Schaeffer and J. Raynal (unpublished); modified by W. Bauhoff.
- 12) C. Olmer, A.D. Bacher, G.T. Emery, W.P. Jones, D.W. Miller, P. Schwandt, T.E. Drake, R.J. Sobie, and S. Yen, to be published; C. Olmer, AIP Conf. Proc., The Interaction between Medium Energy Nucleons in Nuclei, (McCormick's Creek State Park), Spencer, Indiana, to be published.
- 13) W.G. Love in the The (p,n) Reaction and the Nucleon-Nucleon Force, edited by C. Goodman et al., (Plenum, New York, 1980), p. 23.